Table 1-1. *Parametric Uncertainties for Higgs Width Branching Ratio Determination*

Parameter	Central Value	Uncertainty
$\alpha_s(M_Z)$	0.119	$\pm$0.002(90% CL)
m_c	1.42 GeV	$\pm$0.03 GeV(2σ)
m_b	4.49 GeV	$\pm$0.06 GeV(2σ)
m_t	172.5 GeV	$\pm$2.5 GeV

1.2 Coupling Measurements

The central question about the particle discovered at 126 GeV is whether this is "The Higgs Boson" or only one degree of freedom of a bigger story. If there is more than one Higgs boson, and theories such as supersymmetry require there to be multiple bosons at the TeV scale, then the couplings of the 126 GeV boson to matter will not directly correspond to the coupling strengths predicted from the masses of the elementary particles. Additional parameters that describe the mixing of multiple Higgs boson states, or the ratio of vacuum expectation values, or in general the effects of additional degrees of freedom in the Higgs sector will result in deviations in the coupling measurements relative to Standard Model expectations. This is especially true of the loop-induced decays and production modes of the 126 GeV boson where new particles can enter the loops.

The precisions that can be obtained on the coupling measurements are projected for the LHC and e^+e^- machines. A muon collider is expected to be capable of a similar program as the e^+e^- machines, but detector simulations to extract these estimates have not been completed at this time.

1.2.1 Branching Ratio Uncertainties

Extractions of the scaling of Higgs coupling constants from measured decay modes can serve to limit various new physics models, or to confirm the validity of the Standard Model. The conclusions derived from this exercise depend on the uncertainties in the calculation of the Standard Model cross sections and branching ratios. In this subsection, we discuss the uncertainties on the theoretical predictions of the Higgs branching ratios, which have been tabulated by the LHC Higgs cross section working group [**?**, **?**].

There are two types of uncertainties which arise when computing the uncertainties on Higgs branching ratios: parametric uncertainties and theoretical uncertainties. The parametric uncertainties describe the dependence of the predictions on the input parameters. For a 126 GeV Standard Model Higgs boson, the parametric uncertainties arise predominantly from the b mass and α_s and are given in Table 1-1. The parametric uncertainties are combined in quadrature. The theoretical uncertainties are estimated from the QCD scale dependence and from higher order electroweak interactions and given in Table 1-2. The dominant source of the electroweak uncertainty is from NLO corrections which are known, but not included exactly in HDECAY, which is used to determine the uncertainties given here. These electroweak uncertainties can be expected to be reduced in the future. It is also possible that the uncertainty on the b quark mass may be reduced by future lattice calculations.

The total uncertainty is then computed as the linear sum of the parametric and theoretical uncertainties. The final uncertainties on the predictions for the branching ratios for a 126 GeV Standard Model Higgs boson are given in Table 1-3. Ref. [?] also contains the theoretical uncertainties on the predictions for the Higgs total widths, which may be used to include correlations.

Table 1-2. *Theory Uncertainties for $M_H = 126$ GeV Higgs Branching Ratio Determination*

Decay	QCD Uncertainty	Electroweak Uncertainty	Total
$H \to b\bar{b}, c\bar{c}$	$\sim 0.1\%$	$\sim 1-2\%$	$\sim 2\%$
$H \to \tau^+\tau^-, \mu^+\mu^-$	-	$\sim 1-2\%$	$\sim 2\%$
$H \to gg$	$\sim 3\%$	$\sim 1\%$	$\sim 3\%$
$H \to \gamma\gamma$	$< 1\%$	$< 1\%$	$\sim 1\%$
$H \to Z\gamma$	$< 1\%$	$\sim 5\%$	$\sim 5\%$
$H \to WW^*/ZZ^* \to 4f$	$< 0.5\%$	$\sim 0.5\%$	$\sim 0.5\%$

Table 1-3. *Uncertainties on $M_H = 126$ GeV Standard Model Branching Ratio Predictions*

Decay	Theory Uncertainty (%)	Parametric Uncertainty (%)	Total Uncertainty on Branching Ratios (%)
$H \to \gamma\gamma$	± 2.7	± 2.2	± 4.9
$H \to b\bar{b}$	± 1.5	± 1.9	± 3.3
$H \to \tau^+\tau^-$	± 3.5	± 2.1	± 5.6
$H \to WW^*$	± 2.0	± 2.2	± 4.1
$H \to ZZ^*$	± 2.0	± 2.2	± 4.2
$H \to Z\gamma$			

1.2.1.1 Non-Standard Higgs Couplings Due to New Physics

In this section, we survey a few models which can give Higgs couplings different from those of the Standard Model. All of these models contain new particles, so discovery of the new physics can result from direct detection of the new particles, or from the measurement of a deviation in the Higgs coupling from the Standard Model predictions [**?**]. We note that in order to be sensitive to a deviation, δ, the measurement must be made to a precision of roughly $\frac{\delta}{2}$ in order to obtain a 95% confidence level limit, or $\frac{\delta}{5}$ for 5σ.

One Parameter Model

One of the simplest extensions of the Standard Model is to add an $SU(2)$ singlet Higgs, S, which mixes with the usual Higgs doublet, Φ_{SM}, through a mixing term $\mid \Phi_{SM} \mid^2 \mid S \mid^2$. In some scenarios, the singlet, S, could arise from a hidden sector which generates dark matter. There are two mass eigenstate Higgs particles: the observed 126 GeV Higgs boson, h, and a heavier Higgs particle, H. The Standard Model Higgs has couplings which are suppressed relative to the SM values [**?**],

$$\kappa_V \; = \; \kappa_F = \cos\alpha \tag{1.1}$$

where $V = W, Z$ and F denotes all the fermions. The value of $\sin\alpha$ is constrained by precision electroweak data and for $M_H \sim 1$ TeV, we must have $\sin^2\alpha < .12$ [?], which implies that in this model, the target for precision measurements of Higgs couplings is,

$$\kappa_V - 1 = \kappa_F - 1 < 6\ \%\,. \tag{1.2}$$

Two Higgs Doublet Models

One of the most straightforward extensions of the Standard Model is the two Higgs doublet model. The 2HDMs contain 5 physical Higgs bosons: two neutral scalars, h and H, a pseudoscalar, A, and a charged Higgs

Table 1-4. *Light Neutral Higgs, h, Couplings in the 2HDMs*

	I	II	Lepton Specific	Flipped
κ_V	$\sin(\beta-\alpha)$	$\sin(\beta-\alpha)$	$\sin(\beta-\alpha)$	$\sin(\beta-\alpha)$
κ_t	$\frac{\cos\alpha}{\sin\beta}$	$\frac{\cos\alpha}{\sin\beta}$	$\frac{\cos\alpha}{\sin\beta}$	$\frac{\cos\alpha}{\sin\beta}$
κ_b	$\frac{\cos\alpha}{\sin\beta}$	$-\frac{\sin\alpha}{\cos\beta}$	$\frac{\cos\alpha}{\sin\beta}$	$-\frac{\sin\alpha}{\cos\beta}$
κ_τ	$\frac{\cos\alpha}{\sin\beta}$	$-\frac{\sin\alpha}{\cos\beta}$	$-\frac{\sin\alpha}{\cos\beta}$	$\frac{\cos\alpha}{\sin\beta}$

boson, $H^{\pm}$. Models with a Z_2 symmetry can be constructed such that there are no tree-level flavor-changing neutral currents. The couplings of the Higgs bosons to fermions are described by two free parameters; the ratio of vacuum expectation values of the two Higgs doublets, $\tan\beta \equiv \frac{v_2}{v_1}$, and the mixing angle which diagonalizes the neutral scalar mass matrix, α. There are then four possible assignments of couplings for the light CP even Higgs boson, h^0, to fermions and gauge bosons relative to the Standard Model couplings, which are given in Table 1-4. The couplings to W and Z are always suppressed relative to the Standard Model couplings, while in model II and the flipped model, the couplings to $b's$ and τ's are enhanced at large $\tan\beta$.

Current limits on $\tan\beta$ and $\cos(\beta-\alpha)$ [**?**], along with projections for the high luminosity LHC and the $\sqrt{s} = 500$ GeV and $\sqrt{s} = 1000$ GeV ILC (assuming no deviations from the Standard Model) are given in Ref. [**?**]. In model II and the flipped model, $\cos(\beta-\alpha)$ is already constrained to be near one, while larger deviations are possible in model I and the lepton specific model. Large values of $\tan\beta$ are as yet unconstrained by the data.

MSSM
The Higgs sector of the MSSM is a special case of the 2HDM and corresponds to model II. In the MSSM, the mixing angle, α, is related to the masses of the scalars. In the limit where the pseudoscalar A is much heavier than M_Z, the couplings take the simple form (called the decoupling limit) [**?**],

$$\begin{aligned}\kappa_V &\sim 1 - \frac{2M_Z^4}{M_A^4}\cot^2\beta \\ \kappa_t &\sim 1 - \frac{2M_Z^2}{M_A^2}\cot^2\beta \\ \kappa_b = \kappa_\tau &\sim 1 + \frac{2M_Z^2}{M_A^2}\,. \end{aligned} \tag{1.3}$$

Studies of the MSSM suggest that with 3000 fb^{-1} the LHC will be sensitive to $M_A \sim 300$ GeV for all values of $\tan\beta$ not excluded by LEP, giving as a target for the coupling precisions,

$$\begin{aligned}\kappa_V &\sim 1 - .05\%\left(\frac{400\ GeV}{M_A}\right)^4\cot^2\beta \\ \kappa_t &\sim 1 - \mathcal{O}(10\%)\left(\frac{400\ GeV}{M_A}\right)^2\cot^2\beta \\ \kappa_b = \kappa_\tau &\sim 1 + \mathcal{O}(10\%)\left(\frac{400\ GeV}{M_A}\right)^2. \end{aligned} \tag{1.4}$$

For large $\tan\beta$, the Higgs coupling to b's is enhanced and not only is the decay $h \to b\bar{b}$ enhanced, but the dominant production mechanism is the production in association with b's.

New Couplings From Loops
Many models of new physics contain non -Standard Model particles which contribute via loops to the decays $h \to gg$, $h \to \gamma\gamma$ and/or $h \to Z\gamma$,[1] along with altering the $gg \to h$ production rate. These new particles give rise to effective interactions parameterized by κ_g and κ_γ. (Note that the normalization is such that κ_g and $\kappa_\gamma = 1$ in the Standard Model). Generically, one might expect these loop corrections to be $\mathcal{O}\left(\frac{v^2}{M^2}\right) \sim 6\%\left(\frac{1\ TeV}{M}\right)^2$, where M is the scale of the new physics effects. New heavy fermions, such as top partners, and colored scalars can contribute to $h \to gg$ and $h \to \gamma\gamma$, while electrically charged scalars and heavy leptons can contribute to $h \to \gamma\gamma$. Below we examine some representative models, in order to get a feel for the size of the possible effects.

In Little Higgs models with T parity, the couplings scale with the top partner mass, M_T, and assuming the Higgs couplings to Standard Model particles are not changed, the loop induced couplings are [**?**],

$$\kappa_g = \kappa_\gamma \sim 1 - \frac{m_t^2}{M_T^2} \sim 1 - \mathcal{O}(8\%)\left(\frac{600\ GeV}{M_T}\right)^2 . \tag{1.5}$$

In this scenario the production rate from gluon fusion is suppressed, as is the width into $\gamma\gamma$. Adding a vector-like $SU(2)$ doublet of heavy leptons does not change the $gg \to h$ production rate, but can give an enhancement in κ_γ of order $\sim 20\%$, but with large Yukawa couplings required [**?**].

Colored scalars, such as the stop particle in the MSSM, also contribute to both κ_g and κ_γ. If we consider two charge- $\frac{2}{3}$ scalars as in the MSSM, then for the stop much heavier than the Higgs boson,

$$\kappa_g = \kappa_\gamma \sim 1 + \frac{1}{4}\left(\frac{m_t^2}{m_{\tilde{t}_1}^2} + \frac{m_t^2}{m_{\tilde{t}_2}^2} - \frac{m_t^2 X_t^2}{m_{\tilde{t}_1} m_{\tilde{t}_2}}\right) \sim 1 + \mathcal{O}(17\%)\left(\frac{300\ GeV}{m_{\tilde{t}}}\right)^2 \text{ (for } X_t = 0), \tag{1.6}$$

where $X_t = \mid A_t - \mu \cot\beta \mid$ is the stop mixing parameter. If $X_t = 0$, the Higgs couplings to gluons and photons are always increased. If the stops are light, and the mixing is small, large enhancements are possible. In the MSSM, there are other loop contributions to the $h\gamma\gamma$ and hgg couplings which have been extensively studied. Enhancements in the $h \to \gamma\gamma$ coupling can be obtained with light staus and large mixing, with effects on the order of $\sim 25\%$ [**?**].

1.2.2 Theory Uncertainties on LHC Higgs Production

The LHC does not measure Higgs branching ratios, but rather measures the product of production cross section times branching ratio. Assuming the narrow width approximation, the LHC measures,

$$\sigma \cdot BR(ii \to h \to XX) = \frac{\sigma_{ii}\Gamma_{XX}}{\Gamma_H} . \tag{1.7}$$

The LHC cannot measure the total Higgs decay width, Γ_H, with better than $\mathcal{O}(100\%)$ precision (see Sec. 1.5.1). Both production and decay are affected by changes in the Higgs couplings from their Standard Model values.

We parameterize the couplings in terms of deviations from the Standard Model predictions,

$$\begin{aligned} L \;=\; & \Sigma_i \kappa_i \frac{M_i}{v} \overline{f}_i f_i h + \kappa_W g M_W W^{+\mu} W_\mu^- h + \kappa_Z \frac{g M_Z}{\cos\theta_W} Z^\mu Z_\mu h \\ & + \kappa_g \frac{\alpha_s}{12\pi v} h G^{A,\mu\nu} G^A_{\mu\nu} + \kappa_\gamma \frac{2\alpha}{9\pi v} h F_{\mu\nu} F^{\mu\nu} , \end{aligned} \tag{1.8}$$

[1] We do not discuss $h \to Z\gamma$ here, although it can receive significant corrections in new physics models.

Table 1-5. *Theory Uncertainties for $M_H = 125$ GeV Higgs Production at the LHC [?]*

Process	Cross Section (pb)
Gluon fusion	$49.85^{+19.6\%}_{-14.6\%}$
VBF	$4.18^{+2.8\%}_{-3\%}$
hW	$1.504^{+4.1\%}_{-4.4\%}$
hZ	$.883^{+6.4\%}_{-5.5\%}$

where κ_γ and κ_g parameterize the effects of new particles not present in the Standard Model. In the Standard Model, $\kappa_f = \kappa_W = \kappa_Z = 1$ and $\kappa_g = \kappa_\gamma = 1$ in the heavy fermion limit of the Standard Model and f runs over all the charged fermions. We expect that $\kappa_W \sim \kappa_Z$, since non-equal values would break isospin. The cross sections and decay partial widths then scale with the appropriate values of κ_i^2.

The uncertainty on Higgs production has been studied by the LHC Higgs cross section working group for the various channels and is summarized in Table 1-5 [**?**]. These uncertainties must be included in extractions of the scale factors κ_i from LHC data. The error includes factorization/renormalization scale uncertainty and the correlated uncertainty from α_s and the PDF choice, which are added linearly. The scale uncertainty on the gluon fusion rate is $\sim \pm 10\%$, which can potentially be significantly reduced with the inclusion of recent approximate NNNLO results [**?**]. In addition, there are further uncertainties from binning the Higgs data into $0, 1$ and 2 jet bins. The theory error on the 1 jet bin will be significantly reduced with the inclusion of the NNLO result for Higgs plus one jet [**?**] and by resumming jet veto effects.

1.2.3 Measurements at Hadron Colliders and Projections at LHC

In hadronic collisions, the Higgs boson can be produced through the following four main processes: gluon-gluon fusion $gg \to H$ through a heavy quark triangular loop (ggF), vector boson fusion (VBF), associated production with a vector boson W or Z (VH), and production in association with top quarks ($t\bar{t}H$). Representative leading-order diagrams of these processes are shown in Fig. **??**. The production cross sections of these processes at the LHC at $\sqrt{s} = 7, 8$ and 14 TeV are listed in Table 1-6.

$\sqrt{s}$	Cross sections in pb $m_H = 125$ GeV				
(TeV)	ggF	VBF	WH	ZH	ttH
7	15.1	1.22	0.579	0.335	0.086
8	19.5	1.58	0.697	0.394	0.130
14	49.9	4.18	1.50	0.883	0.611

Table 1-6. *Higgs boson production cross sections of different processes at 7, 8 and 14 TeV of pp collisions. These cross sections are taken from Ref.[LHC XS group].*

Since the discovery of the ∼126 GeV Higgs-like particle in Summer 2012, the LHC experiments have focused on the measurements of its production rates and couplings. Both ATLAS and CMS have made public results based on the LHC Run 1 dataset of ∼5 fb^{-1} at 7 TeV and ∼20 fb^{-1} at 8 TeV. These results strongly suggest that the new particle is a Higgs boson and its properties are consistent with the expectations of the SM Higgs boson. After a two-year shutdown, LHC is scheduled to operate again in 2015 at $\sqrt{s} = 14$ TeV. It is expected to deliver 300 fb^{-1} to each experiment by 2022. With the planned high luminosity upgrade, an integrated luminosity of 3000 fb^{-1} is foreseen by 2030. The increased luminosity will significantly increase

the measurement precision of the Higgs boson properties. The current results are briefly summarized and the projected precisions are presented below.

1.2.3.1 Production Rates and Coupling Fits

The rates of Higgs boson productions and decays are parametrized using strength parameters μ defined as the ratios between the observed rates and the expected ones in the standard model:

$$\mu = \frac{\sigma \times BR}{(\sigma \times BR)_{\rm SM}}$$

Table 1-7 summarizes the current measurements of overall rates from the Tevatron [**?**], ATLAS [**?**], and CMS [CMS-PAS-HIG-13-005], separated for the five main decay modes. These measurements are generally in good agreements with the SM prediction of $\mu = 1$. In addition to the measurements by decay modes, measurements by production processes have also been done for some processes through categorizing Higgs candidate events. Searches for rare decays of $H \to \mu\mu$ and $H \to Z\gamma$ have also been performed. However, current sensitivities are generally 10 times above the SM expectations.

Decay mode	Tevatron ($m_H = 125$ GeV)	ATLAS ($m_H = 125.5$ GeV)	CMS ($m_H = 125.7$ GeV)
$H \to \gamma\gamma$	$5.97^{+3.39}_{-3.12}$	$1.55 \pm 0.23(\text{stat}) \pm 0.15(\text{syst})$	0.77 ± 0.27
$H \to ZZ$	–	$1.43 \pm 0.33(\text{stat}) \pm 0.17(\text{syst})$	0.92 ± 0.28
$H \to WW$	$0.94^{+0.85}_{-0.83}$	$0.99 \pm 0.21(\text{stat}) \pm 0.21(\text{syst})$	0.68 ± 0.20
$H \to \tau\tau$	$1.68^{+2.28}_{-1.68}$	–	1.10 ± 0.41
$H \to b\bar{b}$	$1.59^{+0.69}_{-0.72}$	–	1.15 ± 0.62
Combined	$1.44^{+0.59}_{-0.56}$	$1.33 \pm 0.14(\text{stat}) \pm 0.15(\text{syst})$	0.80 ± 0.14
$BR_{\rm inv}$	–	$< 65\%$ at 95% CL	$< 75\%$ at 95% CL

Table 1-7. *Summary of the measured production rates relative to their SM predictions from hadron colliders by decay channels. The last line shows the upper limit on the branching ratio of Higgs to invisible decays.*

For consistent measurements of Higgs couplings, the Higgs boson production and decay must be analyzed together. The LHC experiments have been performing coupling fits following benchmark parametrizations of Ref. [**?**]. The deviations from the SM are implemented as scale factors of Higgs couplings relative to their SM values. For example, the $gg \to H \to \gamma\gamma$ rate can be written as

$$\sigma \times BR(gg \to H \to \gamma\gamma) = \sigma_{SM}(gg \to H) \cdot BR_{SM}(H \to \gamma\gamma) \cdot \frac{\kappa_g^2 \cdot \kappa_\gamma^2}{\kappa_H^2}$$

where κ_g and κ_γ are effective scale factors for Hgg and $H\gamma\gamma$ couplings through loops and κ_H^2 is the scale factor for the Higgs width:

$$\kappa_H^2 = \sum_X \kappa_X^2 BR_{SM}(H \to XX)$$

where κ_X is the scale factor for HXX coupling and $BR_{SM}(H \to XX)$ is the SM value of the $H \to XX$ decay branching ratio. The summation runs over all decay modes in the SM. Non-SM Higgs decay modes

will modify the total Higgs decay width and consequently rescale branching ratios of all other known decays. If BR_{BSM} is the total branching ratio of beyond-standard-model (BSM) decay modes, then κ_H^2 is modified

$$\kappa_H^2 = \sum_X \kappa_X^2 \frac{BR_{SM}(H \to XX)}{1 - BR_{BSM}}$$

Given the current statistics, fits to Higgs couplings to individual leptons, quarks and vector bosons are not meaningful and therefore have not been done so far. However fits have been performed with reduced number of parameters under various assumptions. Results of these fits can be found in Ref. [?] [+ CMS-PAS-HIG-13-005] and Fig. 1-1 illustrates some representative results.

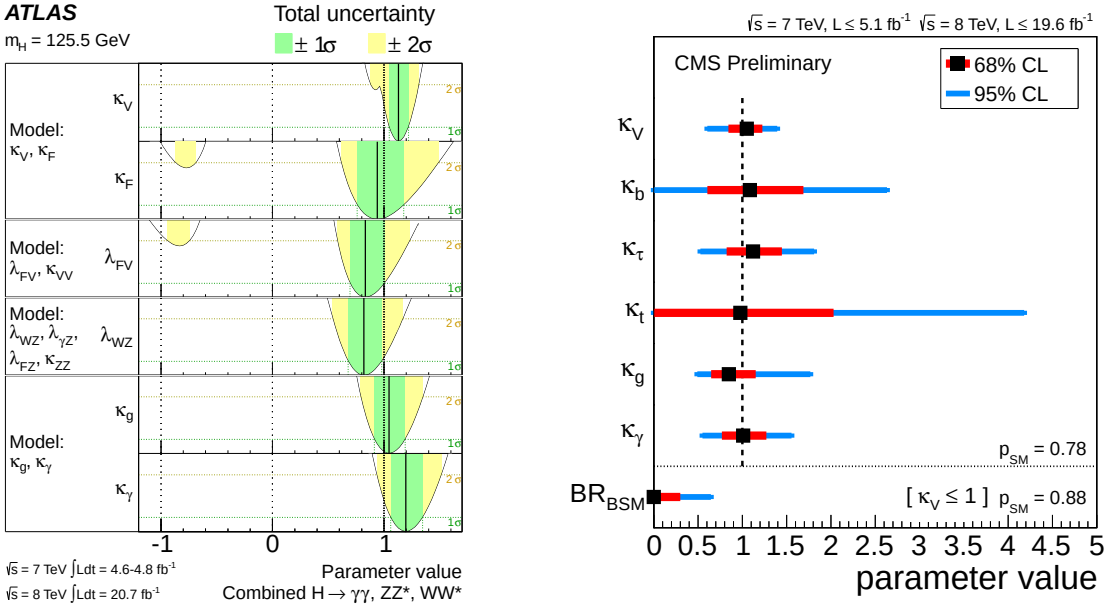

Figure 1-1. *Left: summary of the ATLAS coupling scale factor measurements for different models. The solid vertical lines are the best-fit values while the dark- and light-shaded band represent the total $\pm 1\sigma$ and $\pm 2\sigma$ uncertainties. The curves are distributions of the likelihood ratios. Right: summary of the CMS fits for deviations in the coupling for the generic six-parameter model including effective loop couplings. The result of the fit when extending the model to allow for beyond-SM decays while restricting the coupling to vector bosons to not exceed unity ($\kappa_V \leq 1.0$) is also shown.*

1.2.3.2 LHC Projections

Precision measurements of the properties of the Higgs boson will be a central topic for the LHC physics program in the foreseeable future. The high-luminosity LHC is not only an energy frontier machine, it is also an intensity frontier collider. The expected large statistics will significantly improve the precision of the current measurements of couplings to fermions and vector bosons.

The LHC is expected to deliver 300 fb^{-1} at 14 TeV before the high-luminosity upgrade and 3000 fb^{-1} afterward, representing factors of 15 and 150 increases in statistics from luminosity alone from the current

	ggF	VBF	VH	$t\bar{t}H$	Total
Cross section (pb)	49.9	4.18	2.38	0.611	57.1
			Numbers of events in 3000 fb^{-1}		
$H \to \gamma\gamma$	344,310	28,842	16,422	4,216	393,790
$H \to ZZ^* \to 4\ell$	17,847	1,495	851	219	20,412
$H \to WW^* \to \ell\nu\ell\nu$	1,501,647	125,789	71,622	18,387	1,717,445
$H \to \tau\tau$	9,461,040	792,528	451,248	115,846	10,820,662
$H \to b\bar{b}$	86,376,900	7,235,580	4,119,780	1,057,641	98,789,901
$H \to \mu\mu$	32,934	2,759	1,570	403	37,667
$H \to Z\gamma \to \ell\ell\gamma$	15,090	1,264	720	185	17,258
$H \to$ all	149,700,000	12,540,000	7,140,000	1,833,000	171,213,000

Table 1-8. *The numbers of predicted Higgs events produced in 3000 fb^{-1} at 14 TeV in different production mode and decay channels for $m_H = 125$ GeV. Here $\ell = e, \mu$.*

7 and 8 TeV datasets. The higher pp collision energy will also increase the Higgs production cross sections by a factor of 2.6 or larger. The numbers of predicted Higgs events are shown in Table 1-8.

Both ATLAS and CMS experiments have projected their sensitivities to high luminosities with varying assumptions of detector and analysis performance. Arguably the most significant challenge is to deal with the high pileup that will come along with the high luminosity. The average number of interactions per beam crossing is expected to reach 140 compared with current 20. However, the upgraded detectors are expected to mitigate the adverse impact from the higher pileup and maintain (in some cases exceed) the performance of the current detectors.

ATLAS has taken the approach to estimate sensitivities using fast parametric simulations. Effectively all analyses will have to be repeated and consequently it takes longer to converge. At the time of this report writing, not all major analyses have converged. On the other hand, CMS has taken a different approach, making projections based on the analyses of 7 and 8 TeV data with varying assumptions. Unless noted, CMS projections are taken as the expected LHC per-experiment precisions. Table 1-9 summarizes the expected precisions on the signal strengths of different Higgs decay modes as well as 95% CL upper limit on the branching ratio of Higgs to invisible decay Ref.[CMS white paper]. These projections are based on the analysis of 7 and 8 TeV data, not all final states have been explored. They are expected to improve once more final states are included. Two scenarios of systematics are considered. The first one, conservative scenario, assumes no reduction in systematics as the integrated luminosity is increased. The second one, optimistic scenario, assumes the theoretical systematics are reduced by a factor of two while experimental systematics scale with the inverse of the square-root of the luminosity, i.e., $1/\sqrt{\mathcal{L}}$. These two scenarios bookend the ranges of the projections in the table.

Table 1-10 summarizes the expected precision for two assumptions of systematic uncertainties from fits to a generic 7-parameter model. The 7 parameters are κ_γ, κ_g, κ_W, κ_Z, κ_t, κ_b and κ_τ. In this parameter set, κ_γ and κ_g parametrize potential new physics in loops. κ_t, κ_b and κ_τ parametrize deviations to up-and down-type quarks and charged leptons, respectively. Only SM decays are considered in the fit. The fit is

$\int \mathcal{L}dt$ (fb^{-1})	$H \to \gamma\gamma$	$H \to WW$	$H \to ZZ$	$H \to b\bar{b}$	$H \to \tau\tau$	$H \to Z\gamma$	BR_{inv}
300	$(6-12)\%$	$(6-11)\%$	$(7-11)\%$	$(11-14)\%$	$(8-14)\%$	$(62-62)\%$	$< (17-28)\%$
3000	$(4-8)\%$	$(4-7)\%$	$(4-7)\%$	$(5-7)\%$	$(5-8)\%$	$(20-24)\%$	$< (6-17)\%$

Table 1-9. *Expected relative precisions on the signal strengths of different Higgs decay final states as well as the 95% CL upper limit on Higgs branching ratios to invisible decays. The ranges represent two scenarios of systematic uncertainties, see text.*

extended to allow for BSM decays while restricting the Higgs coupling to vector bosons not to exceed their SM values ($\kappa_W, \kappa_Z \leq 1$). The upper limit on the branching ratio of BSM decay is also included in the table.

As shown in the table, the expected precision ranges from $(5-15)\%$ for 300 fb^{-1} and $(2-10)\%$ for 3000 fb^{-1}. They are limited by systematic uncertainties, particularly theoretical uncertainties on production rates. Statistical uncertainties are below one percent.

Coupling parameter	300 fb^{-1}	3000 fb^{-1}
κ_γ	$(5-7)\%$	$(2-5)\%$
κ_g	$(6-8)\%$	$(3-5)\%$
κ_W	$(4-6)\%$	$(2-5)\%$
κ_Z	$(4-6)\%$	$(2-4)\%$
κ_t	$(14-15)\%$	$(7-10)\%$
κ_b	$(10-13)\%$	$(4-7)\%$
κ_τ	$(6-8)\%$	$(2-5)\%$
$\kappa_{Z\gamma}$	$(41-41)\%$	$(10-12)\%$
κ_μ		
BR_{BSM}	$< (14-18)\%$	$< (7-11)\%$

Table 1-10. *Expected per-experiment precision of Higgs boson couplings to fermions and vector bosons with 300 fb^{-1} and 3000 fb^{-1} integrated luminosity. The range represents spread from conservative and optimistic scenarios, see text.*

ATLAS studies are similar to the conservative scenario. The results are indeed in good agreements with the CMS projections. **will add some text discussing white paper submission from individuals.** some text on rare decays such as $H \to \mu\mu$, $H \to Z\gamma$ and also on invisible width.

1.2.4 Projections for e^+e^- machines

The measurements of Higgs couplings in e^+e^- collisions benefit from a clean experimental environment, precisely known E_{cm} and initial state polarization, and well predicted backgrounds many orders of magnitude below the challenging QCD backgrounds of the hadron colliders. The e^+e^- collider is a well-studied Higgs factory. Although most studies in the past decade focus on linear colliders [**?**], the experimentally accessible Higgs physics at a given center-of-mass energy depends only weakly whether it is a linear or circular machine [**?**, **?**], with differences driven primarily by luminosity and possible number of detector interaction points. In the measurement of Higgs couplings at a linear collider, the very small beam size at

the interaction point and time structure of the beams allowing vertex detectors to be operated in a pulsed mode would benefit flavor tagging in $h \to b\bar{b}$ and $c\bar{c}$ decays. Beamstrahlung effects, resulting in collisions at less than $2E_{\rm beam}$, tend to be less in a circular e^+e^- machine than at a linear collider, although the impact on Higgs precision measurements is small.

The measurement of couplings naturally divides according to the production of process. At relatively low $\sqrt{s}$ energies of $\simeq$ 250 – 350 GeV, the Higgs-strahlung process $e^+e^- \to Zh$ dominates and tagging the Z allows for a model-independent separation of the recoil Higgs decays. For $\sqrt{s} \geq 500$ GeV, the W-fusion mode $e^+e^- \to \nu_e\bar{\nu}_e h$ dominates and grows with $\sqrt{s}$ allowing for better precision of the WW coupling and higher statistics for other decay modes, including rare decays. These higher energies also provide access to the top quark Yukawa coupling through $e^+e^- \to tth$ and the Higgs trilinear self-coupling via double-Higgs production: $e^+e^- \to Zhh$ and $\nu_e\bar{\nu}_e hh$ (discussed in Chapter 1.3.2).

1.2.4.1 Collision energies 250 – 350 GeV

A key decay mode is $e^+e^- \to Zh$ where events can be detected inclusively, completely independent of the Higgs decay mode by tagging the Z via $Z \to \mu^+\mu^-$ and e^+e^- and requiring that the recoil mass is consistent with the Higgs boson mass. The normalization of this rate then allows a precision measurement of $\sigma(Zh)$ that is in turn proportional to g^2_{ZZ}. With this in hand, the other Z decay modes can be employed and measurements of $\sigma(Zh) \cdot \mathcal{B}$ lead to *absolute* measurements of *all* possible branching fractions, including invisible Higgs decays and decay modes undetectable at the LHC due to large backgrounds. Note that the uncertainty on $\sigma(ZH)$ at $\sqrt{s} = 250$ GeV eventually limits the precisions on the branching fraction measurements. Assuming a single resonance,

$$\Gamma_h = \Gamma(h \to ZZ)/\mathcal{B}(h \to ZZ) \propto \sigma(ZH)/\mathcal{B}(h \to ZZ) \tag{1.9}$$

allowing a model independent extraction of the width of the Higgs, free from confusion of whether there is new physics in couplings or in new decay modes. At increasing $\sqrt{s}$, starting at, e.g., the 350 GeV TLEP or the initial 350 GeV phase of CLIC, there is enough rate in the WW-fusion process so that using:

$$\Gamma_h = \Gamma(h \to WW^*)/\mathcal{B}(h \to WW^*), \tag{1.10}$$

$\Gamma(h \to WW^*)$ can be determined by measuring the cross section for $e^+e^- \to \nu_e\bar{\nu}_e h$, giving another handle on the total Higgs width. This is even more true of the higher energies at 500 GeV and beyond. Such a rich program of Higgs physics can be carried out at any of the e^+e^- machines with sufficient luminosity.

Full simulations of such events in the ILD [**?**] and SiD [**?**] detectors [**?**] have been performed over many years, including all physics backgrounds. Overlays of $\gamma\gamma \to$ hadrons and beam-induced backgrounds have also been included for studies at ILC [**?**, **?**] and most CLIC [**?**] studies. A full simulation of the CMS detector has been used to make projections of precisions attainable at TLEP [**?**, **?**, ?], with extrapolations made for $h \to c\bar{c}$ and gg. Results are collated in Table **??**.

1.2.4.2 Collision energies ≥ 500 GeV

The e^+e^- collisions at $\sqrt{s} \geq 500$ GeV are the exclusive realm of linear colliders (more speculative rings such as the Very Large Lepton Collider (VLLC) with circumferences greater than 100 km are not considered here). At these higher energies, large samples of events from both the WW and ZZ fusion processes lead to improved precision on all the branching fractions, and allow probing of rare decays such as $h \to \mu^+\mu^-$. Equally important, the relation of Eq. 1.10 provides a significantly improved measurement of the total Higgs

width consequently improving the precision on *all* the branching fractions and model-independent extraction of the associated Higgs couplings.

Higher energies also open up the production channel $e^+e^- \to t\bar{t}h$. Significant enhancements of this cross section near threshold due to $t\bar{t}$ bound states [**?**] implies that the measurement of the top Yukawa coupling g_t may already be possible at $\sqrt{s} = 500$ GeV [**?**], but has more sensitivity at the higher energy operating points of the ILC and CLIC where the signal cross section is larger and $t\bar{t}$ background is smaller.

Studies using full simulations of detectors at the ILC and CLIC [?,?,?] result in coupling precisions presented in Table **??**.

1.2.4.3 Model Independent Coupling Fits

To provide a true representation of the lepton-collider potential, as well as a comparison between e^+e^- options on an equal fitting, Table **??** shows the precision on couplings from global fits without any assumptions on or between g_W and g_Z, nor with any assumptions on the saturation of the total width by invisible decays. The inputs to these model-independent fits are taken from Table 1.2.7, and *include the caveats listed there regarding the level of simulations used for projecting the precision of a measured* $\sigma \cdot \mathcal{B}$.

Facility		ILC		ILC(LumUp)	TLEP (4 IP)			CLIC	
Energy (GeV)	250	500	1000	250+500+1000	240	350	350	1400	3000
$\int \mathcal{L}dt$ (fb^{-1})	250	+500	+1000	1150+1600+2500	10000	+1400	500	+1500	+2000
$\Delta\Gamma_h/\Gamma_h$	11%	6.0%	5.6%	2.7%	1.1%	0.6%	9.2%	8.5%	8.4%
$\mathcal{B}_{\rm inv}$	$< 0.69\%$	$< 0.69\%$	$< 0.69\%$	$< 0.32\%$	$< 0.1\%$	$< 0.1\%$	tbd	tbd	tbd
$\mathcal{B}_{\rm exotic}$									
$\Delta g_\gamma/g_\gamma$	18%	8.4%	4.1%	2.4%	1.7%	1.5%	–	5.9%	<5.9%
$\Delta g_{Z\gamma}/g_{Z\gamma}$	?	?	?	?	?	?	?	?	?
$\Delta g_g/g_g$	6.4%	2.5%	1.8%	0.94%	1.1%	0.8%	4.1%	2.3%	2.2%
$\Delta g_W/g_W$	4.8%	1.4%	1.4%	0.65%	0.85%	0.19%	2.6%	2.1%	2.1%
$\Delta g_Z/g_Z$	1.3%	1.3%	1.3%	0.61%	0.16%	0.15%	2.1%	2.1%	2.1%
$\Delta g_\mu/g_\mu$	–	–	16%	10%	6.4%	6.2%	–	11%	5.6%
$\Delta g_\tau/g_\tau$	5.7%	2.5%	2.0%	1.0%	0.94%	0.54%	4.0%	2.5%	<2.5%
$\Delta g_c/g_c$	6.8%	3.0%	2.0%	1.1%	1.0%	0.71%	3.8%	2.4%	2.2%
$\Delta g_b/g_b$	5.3%	1.8%	1.5%	0.75%	0.88%	0.42%	2.8%	2.2%	2.1%
$\Delta g_t/g_t$	–	18%	4.0%	2.5%	NA	13%	–	4.5%	<4.5%

Table 1-11. *Couplings as determined in a completely model-independent fit for different e^+e^- facilities. The CLIC numbers are assuming increased WW cross sections above 1 TeV with $(-0.8, 0)$ polarization of (e^-, e^+) (a factor of approximately 1.8 above the unpolarized case). To add: model-independent determination of $\mathcal{B}(H \to$ exotic$)$ for decays that are undetectable at the LHC.*

Final state	$b\bar{b}$	WW^*	$\tau\tau$	$c\bar{c}$	gg	$\gamma\gamma$	ZZ^*	$Z\gamma$	$\mu\mu$
$\Gamma_{\gamma\gamma} \times \mathrm{BR}(h \to X)$	1%	3%	?	–	–	12%	6%	20%	38%

Table 1-12. *Photon collider precisions on Higgs production rates into various final states X, using 5 years nominal luminosity corresponding to a raw sample of 50,000 $\gamma\gamma \to h$ events, from Ref. [?]. The WW^* analysis includes only leptonic final states and the ZZ^* analysis includes only $llqq$ final states.*

1.2.5 Projections for a photon collider operating on the Higgs resonance

A stand-alone photon collider operating on the Higgs resonance could be constructed using laser Compton backscattering off of e^-e^- beams at $\sqrt{s_{ee}} = 160$ GeV [**?**, **?**, **?**]. The photon collider could measure $\Gamma_{\gamma\gamma} \times \mathrm{BR}(h \to X)$ from event rates in various final states.

Table 1-12 summarizes the anticipated sensitivities to production times decay rates after 5 years of data-taking at the HFiTT concept [?], corresponding to 50,000 raw $\gamma\gamma \to h$ events. **What level of simulation went into these HFiTT numbers?**

Model-independent Higgs coupling extraction is not possible unless input from another collider can be provided. If a model-independent measurement of $\mathrm{BR}(h \to bb)$ from an e^+e^- collider is provided [**with what uncertainty?**], a 2% measurement of $\Gamma_{\gamma\gamma}$ can be obtained [?], corresponding to 1% precision on κ_γ. Combining this with the rate measurement for $\gamma\gamma \to h \to \gamma\gamma$ yields a measurement of the total Higgs width to 13% [?].

1.2.6 Projections for a muon collider operating on the Higgs resonance

A muon collider can produce the Higgs boson as an s-channel resonace, $\mu^+\mu^- \to h \to X$. By scanning the beam energy across the resonance, the Higgs total width can be measured directly (see Sec. 1.5.3). Combinations of production and decay couplings can then be extracted from measurements of the event rates in various final states.

Sensitivities have been studied for an idealized detector design including full simulation in Ref. [**?**]. Important components of the detector are tungsten shielding cones at high rapidity and precise timing to reduce beam-related backgrounds.

The studies in [?] simulated Higgs events and Drell-Yan backgrounds for a beam energy scan over a 60 MeV range centered on the Higgs peak using equal-luminosity scan points separated by 4.2 MeV, for a total integrated luminosity of 1 fb^{-1} ($\sim$ 1 year running at nominal machine parameters). The beam was assumed to have a 4.2 MeV-wide Gaussian energy spread (the beam energy spread should be measurable to high precision using muon precession in the accelerator field). Perfect b-tagging efficiency and purity were assumed. Precisions on the $\mu\mu \to h \to X$ rates are given in Table 1-13.

These rates are proportional to $\mathrm{BR}(h \to \mu\mu) \times \mathrm{BR}(h \to X) \propto \kappa_\mu^2\kappa_X^2/\Gamma_h^2$. Products of couplings $\kappa_\mu\kappa_X$ can be extracted using the direct measurement of the Higgs width Γ_h from the lineshape scan, with an estimated uncertainty $\delta\Gamma_h = 3.6$–8.3% (see Sec. 1.5.3). Model-independent Higgs coupling measurements are not possible unless $\mu\mu \to h \to \mu\mu \propto \kappa_\mu^4/\Gamma_h^2$ can be measured. Making the assumption of generation universality, $\kappa_\mu = \kappa_\tau$, is not of much help because the uncertainty on the $\tau\tau$ final state is $\mathcal{O}(100\%)$.

Updated numbers expected from Ron Lipton, to include ISR

Final state	$b\bar{b}$	WW^*	$\tau\tau$	$c\bar{c}$	gg	$\gamma\gamma$	ZZ^*	$Z\gamma$	$\mu\mu$
$\mu\mu \to h \to X$	?	?	?	?	?	–	–	–	–

Table 1-13. *Muon collider precisions on Higgs production rates into various final states X. These numbers assume a Gaussian beam energy resolution of 4.2 MeV and an energy scan over a 60 MeV range in steps of 4.2 MeV using a total luminosity of 1 fb^{-1}. The rates are proportional to* $\mathrm{BR}(h \to \mu\mu) \times \mathrm{BR}(h \to X) \propto \kappa_\mu^2 \kappa_X^2 / \Gamma_h^2$.

1.2.7 Comparison of Precision at Different Facilities

We have requested precision on rate measurements from proponents of various facilities. Hopefully we will receive sufficient information in time so that we can make our own fits. The tables below are place holders.

	ILC/with LumiUp		CLIC 1.4/3.0 TeV		TLEP (4 IPs)	
	Zh	$\nu\nu h$	$Zh^\ddagger$	$\nu\nu h$	Zh	$\nu\nu h$
Inclusive	2.5/1.2%	–	4.2%‡	–	0.4%	–
$h \to \gamma\gamma$	29-38/16%	7-10/5.4%	–	11%$^{\dagger *}$/tbd	3.0%	tbd
$h \to gg$	7/3.3%	2.3/1.4%	6%†	1.4/1.4%	1.4%	tbd
$h \to ZZ^*$	19/8.8%	4.1/2.6%	tbd	2.3†/1.5%†	3.1%	tbd
$h \to WW^*$	6.4/3.0%	1.6/1.0%	2%†	0.75*/0.5%*	0.9%	tbd
$h \to \tau\tau$	4.2/2.0%	3.5/2.2%	5.7%	2.8%/tbd	0.7%	tbd
$h \to b\bar{b}$	1.2/0.56%	0.32/0.20%	1%†	0.23/0.15%	0.2%	0.4%
$h \to c\bar{c}$	8.3/3.9%	3.1/2.0%	5%†	2.2/2.0%	1.2%	tbd
$h \to \mu\mu$	–	31/20%	–	21$^{\dagger *}$/12%	13%	tbd
$h \to Z\gamma$	N/A	N/A	–	tbd/tbd	N/A	N/A
	$t\bar{t}h$		$t\bar{t}h$		$t\bar{t}h$	
$h \to b\bar{b}$	7.8/4.9%		8%$^{\dagger *}$/tbd		–	

Table 1-14. *Precisions of measured $\sigma \cdot \mathcal{B}$ inputs for e^+e^- Higgs factories for complete programs: ILC/with LumiUp: 250/1150 fb^{-1} at 250 GeV, 500/1600 fb^{-1} at 500 GeV, 1000/2500 fb^{-1} at 1000 GeV; CLIC: 500 fb^{-1} at 350 GeV, 1500 fb^{-1} at 1.4 TeV, 3000^{-1} at 3.0 TeV; TLEP (4 IPs): 10000 fb^{-1} at 240 GeV, 1400 fb^{-1} at 350 GeV. (For ILC, re-arrange to give numbers at each center-of-mass energy?). The CLIC numbers are assuming increased WW cross sections above 1 TeV with $(-0.8, 0)$ polarization of (e^-, e^+) (a factor of approximately 1.8 above the unpolarized case). ‡CLIC at 350 GeV; The numbers marked by '*' are preliminary and the numbers marked by '†' are estimates; they will be updated when full simulation results are available.*

Facility	LHC	HL-LHC	ILC	ILC LumiUP	CLIC	TLEP (4 IPs)
Energy (GeV)	14,000	14,000	250+500+1000	250+500+1000	350+1400+3000	240+350
$\int \mathcal{L}dt$ (fb^{-1})	300/expt	3000/expt	250+500+1000	1150+1600+2500	500+1500+2000	10000+1400
N_H ($\times 10^6$)	17	170	0.37	1.05	2.2	3.2
			Measurement precision			
m_H (MeV)	100	50	35	35	33	7
$\Delta\Gamma_H$	–	–	4.8/1.6/1.2%	tbd	?	0.5%
$\mathrm{BR}_{\mathrm{inv}}$	$< 14-18\%$	$< 7-11\%$	<0.44/0.30/0.26%	tbd	tbd	<0.1%
$\Delta g_{H\gamma\gamma}$	$5-7\%$	$2-5\%$	4.9/4.3/3.3%	tbd	–/5.5/<5.5%	1.5%
$\Delta g_{HZ\gamma}$	$41-41\%$	$10-12\%$	?	?	tbd	tbd
Δg_{Hgg}	$6-8\%$	$3-5\%$	4.0/2.0/1.4%	tbd	3.6/0.79/0.56%	0.79%
Δg_{HWW}	$4-6\%$	$2-5\%$	1.9/0.24/0.17%	tbd	1.5/0.15/0.11%	0.10%
Δg_{HZZ}	$4-6\%$	$2-4\%$	0.44/0.30/0.27%	tbd	0.49/0.33/0.24%	0.05%
$\Delta g_{H\mu\mu}$	update	update	–/–/16%	tbd	–/10/5.2%	6.2%
$\Delta g_{H\tau\tau}$	$6-8\%$	$2-5\%$	3.3/1.9/1.4%	tbd	3.5/1.4/<1.3%	0.51%
Δg_{Hcc}	–	–	4.7/2.5/2.1%	tbd	3.1/1.1/0.75%	0.69%
Δg_{Hbb}	$10-13\%$	$4-7\%$	2.7/0.94/0.69%	tbd	1.7/0.32/0.19%	0.39%
Δg_{Htt}	$14-15\%$	$7-10\%$	14/9.3/3.7%	tbd	–/4.0/<4.0%	13%
Δg_{HHH}	–	50%	26%	16%	16/10%	–

Table 1-15. *Expected precisions from measurements and global fits. Values for e^+e^- global fits done with same assumptions as LHC, i.e., assuming* only *SM decay modes. The CLIC numbers are assuming increased WW cross sections above 1 TeV with $(-0.8, 0)$ polarization of (e^-, e^+) (a factor of approximately 1.8 above the unpolarized case). Results for* 9-parameter *fit results, i.e., where $\kappa_t \neq \kappa_c$, and $\kappa_\tau \neq \kappa_\mu$. Break up number of h's into energies.*

Facility	LHC	HL-LHC	ILC**-update	ILC LumiUP	CLIC	TLEP (4 IPs)
Energy (GeV)	14,000	14,000	250+500+1000	250+500+1000	350+1400+3000	240+350
$\int \mathcal{L}dt$ (fb^{-1})	300/expt	3000/expt	250+500+1000	1150+1600+2500	500+1500+2000	10000+1400
N_H ($\times 10^6$)	17	170	0.37	1.05	2.2	3.2
			Measurement precision			
m_H (MeV)	100	50	35	35	33	7
$\Delta\Gamma_H$	–	–	4.8/1.6/1.2%	tbd	8.4%	0.5%
BR_{inv}	NA	NA	<0.44/0.30/0.26%	tbd	tbd	<0.1%
$\Delta g_{H\gamma\gamma}$	$5.1-6.5\%$	$1.5-5.4\%$	4.9/4.3/3.3%	tbd	–/5.5/<5.5%	1.5%
$\Delta g_{HZ\gamma}$	?	tbd	tbd	tbd	tbd	tbd
Δg_{Hgg}	$5.7-11\%$	$2.7-7.5\%$	4.0/2.0/1.4%	tbd	3.6/0.79/0.56%	0.79%
Δg_{HWW}	$2.7-5.7\%^\dagger$	$1.0-4.5\%^\dagger$	1.9/0.24/0.17%	tbd	1.5/0.15/0.11%	0.10%
Δg_{HZZ}	$2.7-5.7\%^\dagger$	$1.0-4.5\%^\dagger$	0.44/0.30/0.27%	tbd	0.49/0.33/0.24%	0.05%
$\Delta g_{H\tau\tau}$	$5.1-8.5\%$	$2.0-5.4\%$	3.3/1.9/1.4%	tbd	3.5/1.4/<1.3%	0.51%
Δg_{Hbb}	$6.9-15\%$	$2.7-11\%$	2.7/0.94/0.69%	tbd	1.7/0.32/0.19%	0.39%
Δg_{Htt}	$8.7-14\%$	$3.9-8.0\%$	14/9.3/3.7%	tbd	3.1/1.0/0.7%	13%
Δg_{HHH}	–	$30\%^\ddagger$	26%	16%	16/10%	–

† assuming the same deviation for the HWW and HZZ couplings. ‡ two experiments.

Table 1-16. *Expected precisions from measurements and global fits. LHC results still have custodial symmetry assumed – results without it will be supplied. Values for e^+e^- global fits done with same assumptions as LHC, i.e., assuming* only *SM decay modes. The CLIC numbers are assuming increased WW cross sections above 1 TeV with $(-0.8, 0)$ polarization of (e^-, e^+) (a factor of approximately 1.8 above the unpolarized case). Results for* 7-parameter *fit results where $\kappa_t = \kappa_c$, and $\kappa_\tau = \kappa_\mu$ for a more direct comparison with LHC default fits. Also for fits across the board allowing invisible decays. Break up number of h's into energies.*

Facility	HL-LHC	LHC	HL-LHC	HL-LHC
		+ ILC/ILC LumiUp	+ ILC LumiUp/TLEP+HE-LHC/TLEP+CLIC	+ HE-LHC/HE-LHC+μC
			Measurement precision	
m_H	50 MeV			
$\Delta\Gamma_H$	–			
$\mathrm{BR}_{\mathrm{inv}}$	NA			
$\Delta g_{H\gamma\gamma}$	$1.5-5.4\%$			
Δg_{Hgg}	$2.7-7.5\%$			
Δg_{HWW}	$1.0-4.5\%^{\dagger}$			
Δg_{HZZ}	$1.0-4.5\%^{\dagger}$			
$\Delta g_{H\mu\mu}$	$< 10\%$			
$\Delta g_{H\tau\tau}$	$2.0-5.4\%$			
Δg_{Hcc}	–			
Δg_{Hbb}	$2.7-11\%$			
Δg_{Htt}	$3.9-8.0\%$			
Δg_{HHH}	$30\%^{\ddagger}$			

† assuming the same deviation for the HWW and HZZ couplings. ‡ two experiments.

Table 1-17. *Comparing precision of measured parameters for combined facilites, using same assumptions in global fits.*